Electron Injection from a Carboxylic Anchoring Dye to TiO$_2$ Nanoparticles in Aprotic Solvents

Hui Fang[1], Yuhao Wu[1], Jianxin Chen[1], Danielle L. Kuhn[2], Zander Zachary[2], Brendan G. DeLacy[2], Yi Rao[1#], and Hai-Lung Dai[1]*

[1]Department of Chemistry, Temple University, Philadelphia, Pennsylvania 19122
[2]U.S. Army Edgewood Chemical Biological Center, Research & Technology Directorate, Aberdeen Proving Ground, Maryland 21010
[#]Present Address: Department of Chemistry and Biochemistry, Utah State University, Logan, Utah 84322

*Corresponding author: hldai@temple.edu

Graphical Abstract
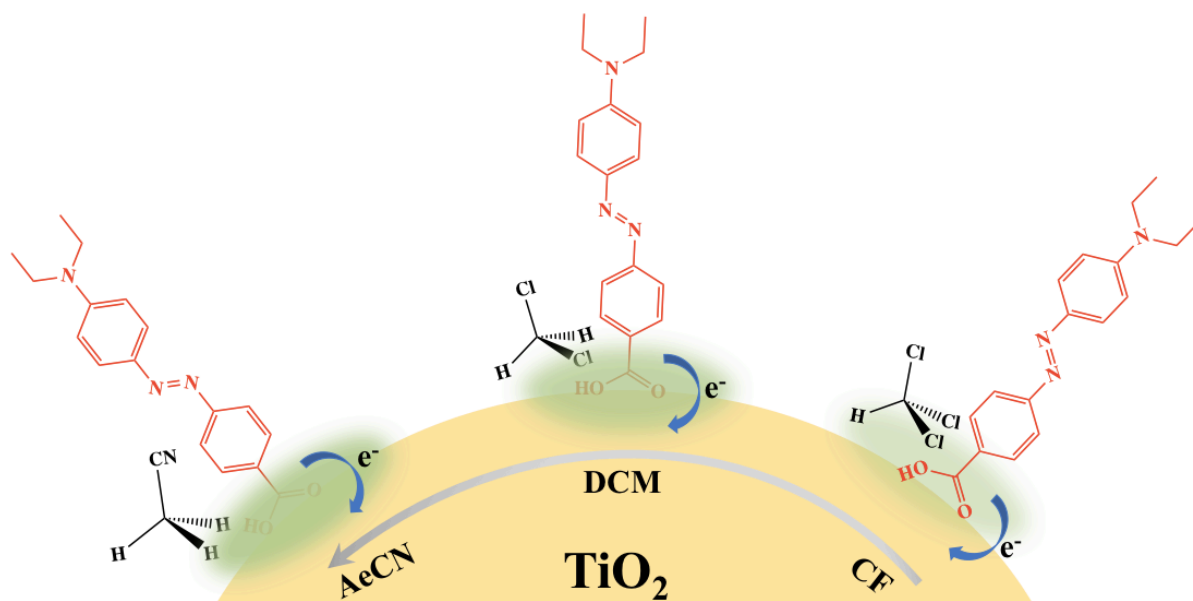
Abstract

Injection of photoexcited electrons in the para-Ethyl Red dye to TiO_2 nanoparticles (Anatase, 40 nm diameter) is characterized by transient absorption on ultrafast time scales. This study focuses on understanding the effect of aprotic solvents on the injection rate. Transient absorption at 1900 cm^{-1} is probed following a 400 nm pulse which excites the electronic transition of p-ER adsorbed on TiO_2 through its carboxylic group. Measurements conducted in three different solvents show that electron injection lifetimes are in the 250-300 fs range but display a trend in correlation with solvent polarity: the electron injection lifetime is the shortest (257 fs) in acetonitrile followed by dichloromethane (271 fs) and chloroform (296 fs). This trend can be understood by using the Marcus theory in which the reorganization energy varies correspondingly in the three different solvents. This study shows that for aprotic solvents the one with the highest polarity facilitates the fastest electron injection.

Keywords

1. Introduction

Understanding interfacial electron injection from molecular adsorbates to semiconductor nanoparticles is a fundamental problem important for improving the efficiency of photocatalytic and photovoltaic processes in systems consisting of semiconductor nanoparticles coated with light absorbing molecules [1-5]. One of the systems of current interests is the dye sensitized solar cell (DSSC) in which a typical device contains TiO_2 particles adsorbed with organic dye molecules[6, 7]. So far, the highest efficiency reported for the DSSC is 13% [8]. One of the approaches to improve the efficiency is to understand what the factors are influencing the injection of photo-generated excited carriers in the organic dye molecules into the TiO_2 particles as the basis for better design. Typically a high DSSC efficiency depends on fast carrier injection and slow recombination[5, 9-13].

Many factors affect the electron injection dynamic process. These factors include the relative energies of the electronic bands of the molecule and the semiconductor, the coupling between the molecular and semiconductor wavefunctions, and the interfacial environment including the surrounding solvent molecules. There have been studies in recent years on the electron injection rate in systems relevant to DSSC[9, 13-19]. Specifically, the solvent

effect has been studied though the understanding is still being formed [9, 15, 16, 18].

In principle, the solvent may affect the band edge position of the semiconductor, its electronic coupling with the adsorbate molecules, and the energy of the molecules before and after the injection. The many reports so far have provide abundant information for characterizing the injection process but our knowledge on how the presence of solvent molecules may affect carrier injection dynamics is still evolving. Lian and coworkers reported that the presence of aqueous water or protic solvents like methanol and ethanol lowers the band edge of TiO_2 and increases the electron injection rate from the light absorbing dye to TiO_2 [15]. They have also investigated the pH dependence of electron injection from the perspective of the change of the band edge position [16]. Ellis et al reported that the nonpolar solvent like hexane has negligible influence on charge transfer dynamics from quantum dots [20]. Durrant et al found that solvents, either protic or aprotic, do not significantly affect the electron injection rates in $Ru(dcbpy)_2(NCS)_3/TiO_2$ films [21]. In contrast, Lee et al discovered that the donor number rather than the dielectric constant of the solvent matters more to the electron injection rate [22]. Hyun et al found that the charge transfer rate increases dramatically with solvent dielectric constant

which was accounted for by a modified Marcus theory taking into account only the static dielectric effect [23].

In this study, we examine if there is a systematic dependence in the electron injection rate upon the change of solvent among the aprotic solvents. In the aprotic solvents there is a lack of hydrogen bonding for the dye molecules. We have previously found that the adsorption free energy is affected by the polarity of the aprotic solvent, likely due to the change in the solvation energy[24]. In principle the change in solvent molecule polarity may affect the solvent interaction with both the semiconductor and the adsorbate and subsequently the injection rate.

The electron transfer (ET) dynamics at the adsorbate-semiconductor nanoparticle interface in an aprotic solvent in this study was probed by transient absorption spectroscopy which has been widely used for probing electron dynamics [5, 11, 15, 16, 20, 23, 25-30]. Following the laser-pulse excitation of the adsorbate electronic transition, an IR laser pulse probes the absorption through intraband transitions of the electrons in the conduction band of the semiconductor [28]. For the free carrier to absorb a photon, scattering with a phonon is required for momentum conservation, resulting in an absorption coefficient that increases with the photon wavelength. Consequently absorption

by free carriers in the conduction band is strong through the mid-IR but becomes negligible in the visible region.

In our study, we chose 400 nm as the pump and 1900 cm^{-1} as the probe to study the excited-electron injection and decay processes in the system of para-Ethyl Red (p-ER) coated TiO_2 nanoparticles. A 400 nm ultrafast pump pulse excited the electrons in p-ER. The 1900 cm^{-1} ultrafast pulse, with varying time delay, probed the absorption of the excited electrons injected into the conduction band of TiO_2. Three different aprotic solvents (acetonitrile, dichloromethane, and chloroform) were chosen to study the solvent effect on the electron injection rate.

2. Experimental

2.1 Transient Absorption

A regen-amplified Ti:Saphire laser system (Quantronix) operating at 800 nm and 1 KHz repetition rate [34] was used for the experiments. The 800 nm output from the regenerative amplifier was split into two parts to generate pump and probe pulses. A very small portion was frequency doubled in a BBO crystal to generate pump pulses at 400 nm with the fluence at the sample kept as low as 3 μJ/pulse (using a combination of a halfwave plate and a polarizer) to minimize higher-order annihilation processes. The other part of the output laser pulse was

used to pump an IR Optical Parametric Amplifier (Quantronix, Palitra-FS/REV.A) to generate two tunable near-IR pulses in the ranges of 1.2 to 1.5 µm and 2.4 to 1.7 µm, separately. These signal and idler pulses were then combined in a $AgGaS_2$ crystal to generate 1900 cm^{-1} pulses through difference frequency generation. The pump and probe pulse focal point sizes were 350 and 160 µm, respectively. The 1900 cm^{-1} radiation was detected by a liquid nitrogen cooled HgCdTe detector (Judson J15D14-M204B-S01M-60-D31316). The pump pulses were chopped by a New Focus Model 3501 Chopper at 500 Hz so that the absorbance change can be measured as the difference between two adjacent probe pulses (one with pump on and the next without). Signals from the probe detector was sent to a lock-in system (Stanford Research, SR830 DSP Lock-in Amplifier). The digitized outputs were processed and recorded by a home-made program based on Labview. The pump-probe cross correlation was approximated by a Gaussian with FWHM of 300 ± 10 fs.

2.2 Materials

Titanium oxide powders (Anatase TiO_2, 99.9%, 40 nm diameter) were purchased from US Research Nanomaterials Inc. pare-Ethyl Red (p-ER) was synthesized using the procedure reported before [24]. Chloroform (CF, 99.7%) and dichloromethane (DCM, 99.9%) were purchased from Alfa Aesar Inc. Acetonitrile (AeCN, ≥99.93%) were purchased from Sigma-Aldrich. These

solvents were used as received. 0.5 mg/ml TiO_2 particles and 0.37 mM p-ER were prepared as stock solutions which were used for preparing the samples for the transient absorption experiments. For example, the p-ER/TiO_2 in CF solution was mixed with 2 ml TiO_2 stock solution and 2 ml p-ER stock solution.

A 10 mm x 5 mm quartz cuvette (Starna Cells Inc.) was used to host the sample with the short path for light propagation. A 2 mm x 2 mm stirrer (Big Science Inc.) was used to make sure that the colloid solution is uniform during the measurement.

3. Results

Figure 1 shows traces of transient absorption of the IR pulses measured following the pump pulse excitation of the p-ER/TiO_2 nanoparticles in the CF solution. The green line is the solvent response measured for solvent only without the particles or dye as the instrument response function, which is fitted with a Gaussian function with 300 fs FWHM. The blue line displays the measurement for only p-ER in CF. This curve is very similar to the instrument response function and indicates that p-ER molecules in the solution (a relatively high 0.18 mM concentration) do not contribute to the transient absorption signal. The black line represents the transient absorption response from a TiO_2 in CF sample. The rise of the signal corresponds to electron excitation in the

TiO$_2$ nanoparticle by the 400 nm pulse. This observation indicates that electrons of TiO$_2$ can be excited by the 400 nm (3.1 eV) pulse to most likely the trap states below the conduction band of TiO$_2$, as the bandgap of the Anatase TiO$_2$ is nearly 3.2 eV [31]. The decay of the signal is apparently long on the time-scale of display.

The red curve in Figure 1 is the transient absorption response from a p-ER/TiO$_2$ in CF sample. p-ER at 0.18 mM concentration ensures a saturation coverage on the particle surface [29]. The rise corresponds to the electron injection transfer process from the p-ER excited states into the conduction band of the TiO$_2$ particle. The slow decay of the signal observed after electron injection into TiO$_2$ indicates that diffusion as well as recombination of the excited carriers in TiO$_2$ is very long on the time scale of display here. The magnitude of rise in the signals from the p-ER/TiO$_2$ samples is much larger than that from samples with TiO$_2$ only. This observation depicts that the injection following excitation of the dye molecules produces many more excited electrons in TiO$_2$ than direct excitation of the particle itself. As a result, the contribution from the TiO$_2$ absorption is neglected in the following analysis of the p-ER/TiO$_2$ signals.

To investigate the solvent effect on electron injection from p-ER molecules into TiO$_2$, three different solvents, acetonitrile (AeCN), dichloromethane

(DCM), and chloroform (CF), were chosen. The absolute magnitude of the transient absorption ΔA is affected by the p-ER coverage on the particles and the excitation efficiency at 400 nm of p-ER which changes in different solvents. For characterizing the dynamics we focus on the change of the signal in time. The transient absorption ΔA from samples made of these three solvents were plotted in Figure 2. The insert of the figure shows the three traces with the absolute magnitude normalized at their maximum values. The injection rates, obtained from fitting the transient absorption traces to a single exponential rise convoluted with the instrument response function (300 fs), for the three solvents are 257 ± 19 fs (AeCN), 271± 16 fs (DCM), and 296 ± 8 fs (CF) respectively (Table 1).

4. Discussion

The observed injection rates from p-ER to Anatase TiO_2 nanoparticles in the three different aprotic solvents are all in the range of 250-300 fs. This range compares similarly to the <500 fs values reported for p-ER/TiO_2 systems in Ref. [36]. Among the three aprotic solvents, a clear trend emerges: the more polar solvent appears to have a faster electron injection rate.

To understand how different aprotic solvents affect the electron injection rate, it is useful to review the classical Marcus theory which was suggested

previously for understanding electron transfer from the dye molecule to the semiconductor [15]. Here we consider only the parts of the rate equation that are relevant to the solvent. The total Electron Transfer (ET) rate from the adsorbate to the semiconductor using the classical Marcus formulation [15, 32, 33] depends on the coupling between the molecule and the semiconductor, the density of the semiconductor states at the energy of the excited molecular state with respect to the semiconductor band edge, and the energy changes from the initial to the final states. The effect of the solvent appears most prominently in the reorganization energy λ, the change of energy of the system as a result of the change in charge distribution in the electron injection process, of the free energy change. The free energy change due to the different interactions between the semiconductor and the different aprotic solvents is negligible, as evidenced by the negligible change in conduction band edge in different solvents [34].

The reorganization energy consists of the vibrational (λ_i) and the electronic (λ_o) contributions. The vibrational contribution is relatively small in this case of molecular excitation and can be neglected in comparison with the electronic contribution ($\lambda \approx \lambda_o$). The electronic reorganization energy can be calculated from the dielectric response of the solvent to a change in charge distribution from the neutral molecule/semiconductor to a charged ion/charged semiconductor as [32]

$$\lambda_0 = \frac{(\Delta e)^2}{2a}\left(\frac{1}{\varepsilon_1^{op}} - \frac{1}{\varepsilon_1^s}\right) - \frac{(\Delta e)^2}{2R}\left(\frac{1}{\varepsilon_1^{op}}\frac{\varepsilon_2^{op}-\varepsilon_1^{op}}{\varepsilon_2^{op}+\varepsilon_1^{op}} - \frac{1}{\varepsilon_1^s}\frac{\varepsilon_2^s-\varepsilon_1^s}{\varepsilon_2^s+\varepsilon_1^s}\right) \qquad (1)$$

where Δe is the charge difference for the adsorbate before and after electron injection; a is the radius of the dye molecule or the distance to the interface; R is the distance between the center of the molecule and its image in the semiconductor, or twice the distance to the interface ($R=2a$); ε^{op} and ε^s are the high (optical) frequency and static dielectric constants, where $\varepsilon^{op} = n^2$, n being the reflective index of the solvent; and the subscripts 1 and 2 represent the solvent and semiconductor respectively. In this case Δe=1, a=0.4 nm for p-ER, and the other values used are summarized in Table 2 [35]. The reorganization energy for the three different solvents are calculated as 0.48 eV (AeCN), 0.38 eV (DEM), and 0.31 eV (CF). As plotted in Figure 3, these calculated reorganization energies do show a correlation with the measured electron injection rates; the electron transfer rate increase as λ_o increases.

In order to understand the trend in Figure 3, the Marcus theory is examined here. The electron transfer rate constant as expressed in Marcus Theory can be reduced to Equation 2:

$$k_{ET} = A\frac{1}{\sqrt{4\pi\lambda_o k_B T}}exp[-\frac{(\lambda_o+\Delta G)^2}{4\lambda_o k_B T}] \qquad (2)$$

where A is a simplified parameter incorporating integrations over functions that are assumed to be non-variant as the solvent changes; $k_B T$ is the Boltzmann

constant-temperature which in this case is 27.5 meV. In this equation it is clear that with a fixed ΔG value (the best estimate as -1.38 eV [35]), the electron injection rate increases with reorganization energy, i.e. the electron injection rate follows the trend AeCN > DCM > CF.

This study shows that though the difference is not large, still in the aprotic solvent environment, the most polar solvent facilitates the fastest electron injection. Previously we have shown that the most polar aprotic solvent enables the saturation coverage of the dye at lower dye concentrations [24]. This and the previous studies combined points to the suggestion that a more polar solvent like acetonitrile is a better choice for DSSC for higher efficiencies.

5. Conclusion

The aprotic solvent effect on the electron injection rate in p-ER sensitized Anatase TiO_2 colloid solutions have been studied by ultrafast transient IR absorption spectroscopy. The electron injection lifetime from p-ER molecules to the TiO_2 nanoparticles were found in the range of 250-300 fs for the three aprotic solvents. Though the differences are not large, there appears a clear trend that the electron injection rate increases with solvent polarity. This increase can be understood base on the change in the reorganization energy in the Marcus theory formulation of the electron transfer rates. Our results suggest

that in the aprotic solvent environment, the solvent with the largest polarity facilitates the fastest electron injection.

Acknowledgements

Reference

[1] C.S. Ponseca, P. Chábera, J. Uhlig, P. Persson, V. Sundström, Ultrafast Electron Dynamics in Solar Energy Conversion, Chemical Reviews 117 (2017) 10940-11024.

[2] R.J.D.M. Miller, G. L.; Nozik, A. J.; Schmickler, W.; Willig, F. , Surface Electron Transfer Processes VCH Publisher: New York (1995).

[3] J. Moser, M. Graetzel, Photosensitized electron injection in colloidal semiconductors, Journal of the American Chemical Society 106 (1984) 6557-6564.

[4] G. Benkö, J. Kallioinen, J.E.I. Korppi-Tommola, A.P. Yartsev, V. Sundström, Photoinduced Ultrafast Dye-to-Semiconductor Electron Injection from Nonthermalized and Thermalized Donor States, Journal of the American Chemical Society 124 (2002) 489-493.

[5] N.A. Anderson, T. Lian, Ultrafast Electron Transfer At The Molecule-Semiconductor Nanoparticle Interface, Annual Review of Physical Chemistry 56 (2004) 491-519.

[6] A. Hagfeldt, G. Boschloo, L. Sun, L. Kloo, H. Pettersson, Dye-Sensitized Solar Cells, Chemical Reviews 110 (2010) 6595-6663.

[7] B. O'Regan, M. Grätzel, A low-cost, high-efficiency solar cell based on dye-sensitized colloidal TiO2 films, Nature 353 (1991) 737.

[8] S. Mathew, A. Yella, P. Gao, R. Humphry-Baker, B.F.E. Curchod, N. Ashari-Astani, I. Tavernelli, U. Rothlisberger, M.K. Nazeeruddin, M. Grätzel, Dye-sensitized solar cells with 13% efficiency achieved through the molecular engineering of porphyrin sensitizers, Nature Chemistry 6 (2014) 242.

[9] J.B. Asbury, N.A. Anderson, E. Hao, X. Ai, T. Lian, Parameters Affecting Electron Injection Dynamics from Ruthenium Dyes to Titanium Dioxide Nanocrystalline Thin Film, The Journal of Physical Chemistry B 107 (2003) 7376-7386.

[10] D. Kuciauskas, J.E. Monat, R. Villahermosa, H.B. Gray, N.S. Lewis, J.K. McCusker, Transient Absorption Spectroscopy of Ruthenium and Osmium Polypyridyl Complexes Adsorbed onto Nanocrystalline TiO2 Photoelectrodes, The Journal of Physical Chemistry B 106 (2002) 9347-9358.

[11] T.A. Heimer, E.J. Heilweil, C.A. Bignozzi, G.J. Meyer, Electron Injection, Recombination, and Halide Oxidation Dynamics at Dye-Sensitized Metal Oxide Interfaces, The Journal of Physical Chemistry A 104 (2000) 4256-4262.

[12] S.A. Haque, Y. Tachibana, R.L. Willis, J.E. Moser, M. Grätzel, D.R. Klug, J.R. Durrant, Parameters Influencing Charge Recombination Kinetics in Dye-Sensitized Nanocrystalline Titanium Dioxide Films, The Journal of Physical Chemistry B 104 (2000) 538-547.

[13] J.B. Asbury, E. Hao, Y. Wang, H.N. Ghosh, T. Lian, Ultrafast Electron Transfer Dynamics from Molecular Adsorbates to Semiconductor Nanocrystalline Thin Films, The Journal of Physical Chemistry B 105 (2001) 4545-4557.

[14] J. Wiberg, T. Marinado, D.P. Hagberg, L. Sun, A. Hagfeldt, B. Albinsson, Distance and Driving Force Dependencies of Electron Injection and Recombination Dynamics in Organic Dye-Sensitized Solar Cells, The Journal of Physical Chemistry B 114 (2010) 14358-14363.

[15] C. She, J. Guo, T. Lian, Comparison of Electron Injection Dynamics from Re-bipyridyl Complexes to TiO2 Nanocrystalline Thin Films in Different Solvent Environments, The Journal of Physical Chemistry B 111 (2007) 6903-6912.

[16] C. She, N.A. Anderson, J. Guo, F. Liu, W.-H. Goh, D.-T. Chen, D.L. Mohler, Z.-Q. Tian, J.T. Hupp, T. Lian, pH-Dependent Electron Transfer from Re-bipyridyl

Complexes to Metal Oxide Nanocrystalline Thin Films, The Journal of Physical Chemistry B 109 (2005) 19345-19355.

[17] G. Benkö, P. Myllyperkiö, J. Pan, A.P. Yartsev, V. Sundström, Photoinduced Electron Injection from Ru(dcbpy)2(NCS)2 to SnO2 and TiO2 Nanocrystalline Films, Journal of the American Chemical Society 125 (2003) 1118-1119.

[18] T. Hannappel, B. Burfeindt, W. Storck, F. Willig, Measurement of Ultrafast Photoinduced Electron Transfer from Chemically Anchored Ru-Dye Molecules into Empty Electronic States in a Colloidal Anatase TiO2 Film, The Journal of Physical Chemistry B 101 (1997) 6799-6802.

[19] Y. Tachibana, J.E. Moser, M. Grätzel, D.R. Klug, J.R. Durrant, Subpicosecond Interfacial Charge Separation in Dye-Sensitized Nanocrystalline Titanium Dioxide Films, The Journal of Physical Chemistry 100 (1996) 20056-20062.

[20] J.L. Ellis, D.D. Hickstein, K.J. Schnitzenbaumer, M.B. Wilker, B.B. Palm, J.L. Jimenez, G. Dukovic, H.C. Kapteyn, M.M. Murnane, W. Xiong, Solvents Effects on Charge Transfer from Quantum Dots, Journal of the American Chemical Society 137 (2015) 3759-3762.

[21] J.R. Durrant, Y. Tachibana, I. Mercer, J.E. Moser, M. Grätzel, D.R. Klug, The Excitation Wavelength and Solvent Dependance of the Kinetics of Electron

Injection in Ru(dcbpy)2(NCS)2 Sensitized Nanocrystalline TiO2 Films, Zeitschrift für Physikalische Chemie, 1999, pp. 93.

[22] K.-M. Lee, V. Suryanarayanan, K.-C. Ho, Influences of different TiO2 morphologies and solvents on the photovoltaic performance of dye-sensitized solar cells, Journal of Power Sources 188 (2009) 635-641.

[23] B.-R. Hyun, A.C. Bartnik, J.-K. Lee, H. Imoto, L. Sun, J.J. Choi, Y. Chujo, T. Hanrath, C.K. Ober, F.W. Wise, Role of Solvent Dielectric Properties on Charge Transfer from PbS Nanocrystals to Molecules, Nano Letters 10 (2010) 318-323.

[24] H. Fang, B. Xu, X. Li, D.L. Kuhn, Z. Zachary, G. Tian, V. Chen, R. Chu, B.G. DeLacy, Y. Rao, H.-L. Dai, Effects of Molecular Structure and Solvent Polarity on Adsorption of Carboxylic Anchoring Dyes onto TiO2 Particles in Aprotic Solvents, Langmuir 33 (2017) 7036-7042.

[25] T.A. Heimer, E.J. Heilweil, Direct Time-Resolved Infrared Measurement of Electron Injection in Dye-Sensitized Titanium Dioxide Films, The Journal of Physical Chemistry B 101 (1997) 10990-10993.

[26] N.A. Anderson, E. Hao, X. Ai, G. Hastings, T. Lian, Ultrafast and long-lived photoinduced charge separation in MEH-PPV/nanoporous semiconductor thin film composites, Chemical Physics Letters 347 (2001) 304-310.

[27] M. Shim, S.V. Shilov, M.S. Braiman, P. Guyot-Sionnest, Long-Lived Delocalized Electron States in Quantum Dots: A Step-Scan Fourier Transform Infrared Study, The Journal of Physical Chemistry B 104 (2000) 1494-1496.

[28] J.I. Pankove, Optical processes in semiconductors, New York, NY : Dover, (1975).

[29] T.P. Dougherty, E.J. Heilweil, Ultrafast transient infrared absorption studies of $M(CO)_6$ (M=Cr, Mo or W) photoproducts in n-hexane solution, Chemical Physics Letters 227 (1994) 19-25.

[30] J.D. Beckerle, M.P. Casassa, R.R. Cavanagh, E.J. Heilweil, J.C. Stephenson, Ultrafast infrared response of adsorbates on metal surfaces: Vibrational lifetime of CO/Pt(111), Physical Review Letters 64 (1990) 2090-2093.

[31] D.O. Scanlon, C.W. Dunnill, J. Buckeridge, S.A. Shevlin, A.J. Logsdail, S.M. Woodley, C.R.A. Catlow, M.J. Powell, R.G. Palgrave, I.P. Parkin, G.W. Watson, T.W. Keal, P. Sherwood, A. Walsh, A.A. Sokol, Band alignment of rutile and anatase TiO_2, Nature Materials 12 (2013) 798.

[32] R.A. Marcus, Reorganization free energy for electron transfers at liquid-liquid and dielectric semiconductor-liquid interfaces, The Journal of Physical Chemistry 94 (1990) 1050-1055.

[33] M. Tachiya, Generalization of the Marcus equation for the electron-transfer rate, The Journal of Physical Chemistry 97 (1993) 5911-5916.

[34] G. Redmond, D. Fitzmaurice, Spectroscopic determination of flatband potentials for polycrystalline titania electrodes in nonaqueous solvents, The Journal of Physical Chemistry 97 (1993) 1426-1430.

[35] L. Zhang, J.M. Cole, P.G. Waddell, K.S. Low, X. Liu, Relating Electron Donor and Carboxylic Acid Anchoring Substitution Effects in Azo Dyes to Dye-Sensitized Solar Cell Performance, ACS Sustainable Chemistry & Engineering 1 (2013) 1440-1452.

[36] M. Stamate, Lazar, G. & Lazar, I. , Anatase - rutile TiO2 thin films deposited in a d.c. magnetron sputtering system. , Rom. J. Phys. 53 (2008) 217-221.

Table 1 The lifetime of electron injection from p-ER to the TiO_2 particle in different solvents (AeCN, DCM, CF) measured as the rise of the transient absorption signal.

Solvent	Rise time (fs)
AeCN	257 ± 19
DCM	271 ± 16
CF	296 ± 8

Table 2 The refractive index (n), Optical (ε^{op}) and Static Dielectric Constants (ε^{s}); and the calculated Reorganization Energy (λ_o) for the three p-ER/TiO$_2$/Solvent systems.

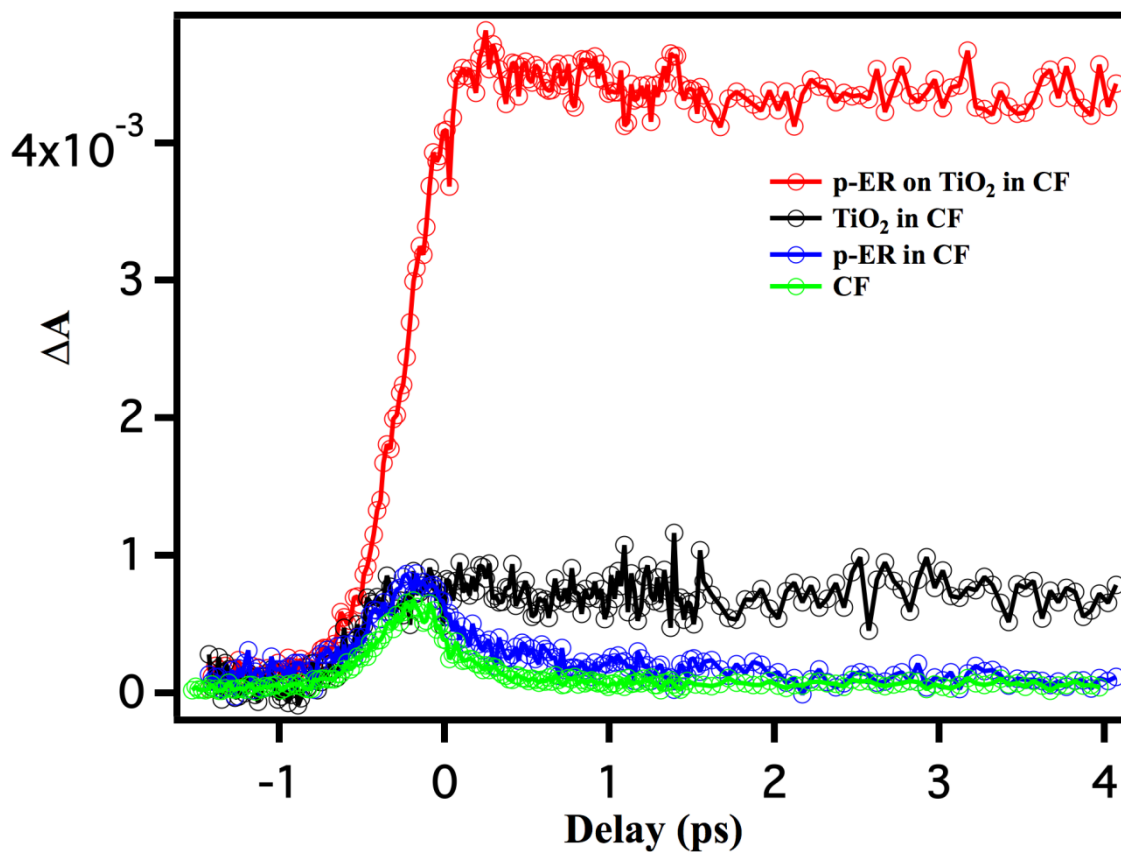| Solvent	n	ε^{op}	ε^{s}	λ_o (eV)
AeCN	1.34	1.81	37.5	0.48
DCM	1.42	2.03	8.93	0.38
CF	1.45	2.09	4.81	0.31
TiO$_2$[a]	2.50	6.25	30	N/A

[a] from Refs. [9, 36]

Fig 1. Transient absorption signal (at 1900 cm^{-1}) following the 400 nm excitation pulse: The green line is obtained with the solvent CF only; the blue line from p-ER in CF; the black line from TiO_2 nanoparticles in CF; and the red curve from p-ER/TiO_2 nanoparticles in CF. t=0 was set as the first maximum point of the red signal.
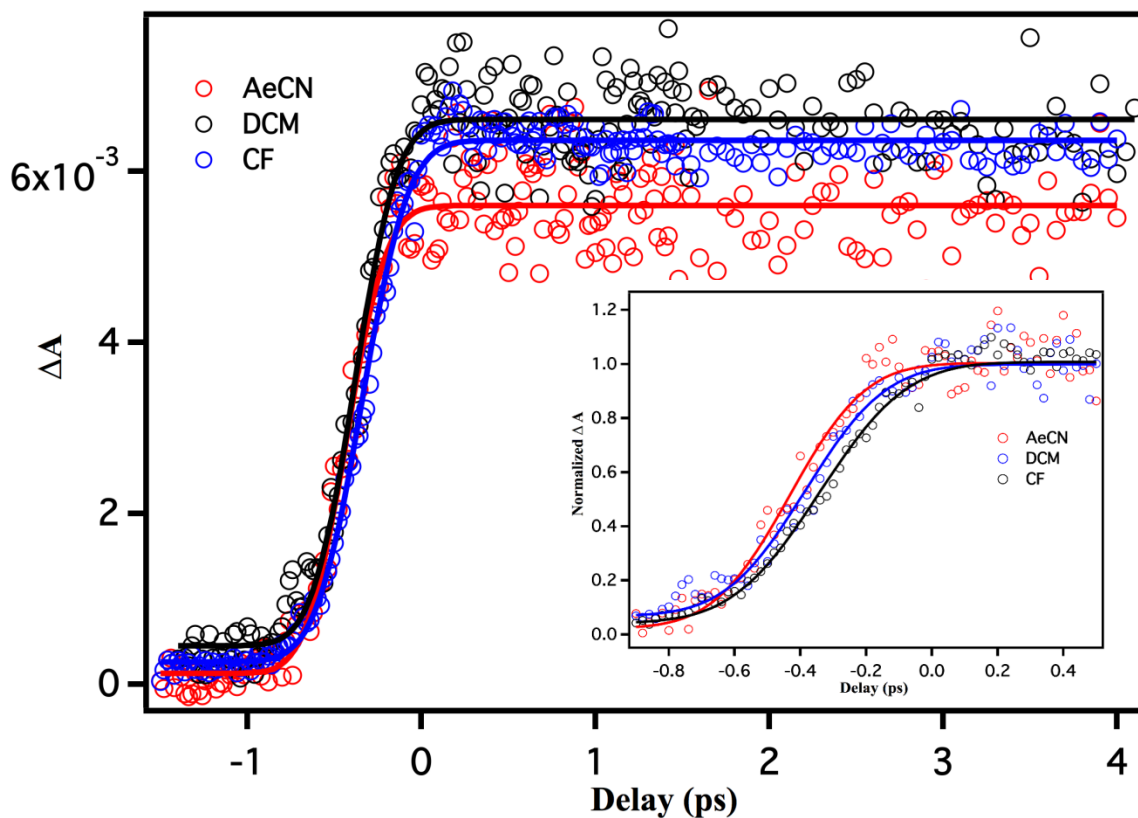
Fig 2. Transient absorption curves obtained from p-ER on TiO_2 nanoparticles in three different solvents (AeCN, DCM, CF) with 400 nm pump and 1900 cm^{-1} probe. The points are measured signals and lines model fittings. Insert shows the early portion of the normalized curves according to the fittings, where the rise of the signals shows the trend of AeCN>DCM>CF.
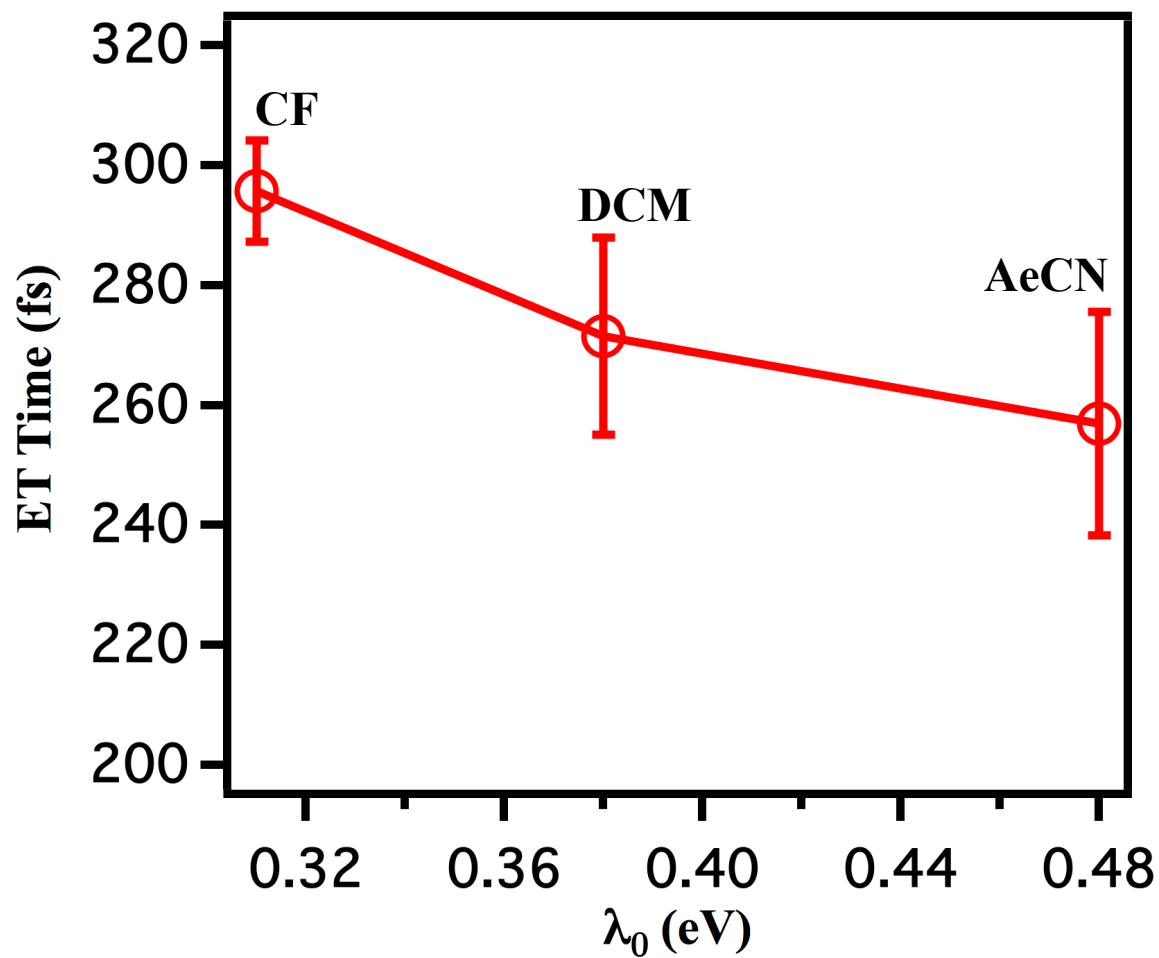
Fig 3. The lifetime of electron injection from p-ER into the TiO_2 nanoparticle in three different solvents (AeCN, DCM, CF) plotted as a function of the calculated Reorganization Energy (λ_o).